VOL. 15, NO. 20, OCTOBER 2020 ISSN 1819-6608
ARPN Journal of Engineering and Applied Sciences

www.arpnjournals.com

CLASSICAL AND ADVANCED CONTROL APPLIED TO A NON-LINEAR LIQUID LEVEL SYSTEM

Andrés Felipe Rojas Suárez, Fredy Camilo Ochoa González and Diego F. Sendoya-Losada
Department of Electronic Engineering, Faculty of Engineering, Surcolombiana University, Neiva, Huila, Colombia
E-Mail: diego.sendoya@usco.edu.co

ABSTRACT

This article illustrates the design of an Internal Model Controller (IMC), used to regulate a non-linear liquid level system. To obtain the design, a transfer function of the system was required, so the model was linearized at an intermediate setpoint. Already obtained, it was compared with a Proportional Integral (PI) controller, in order to verify the performance of each controller for setpoint tracking and disturbance rejection.

Keywords: IMC, Level control, PI, RMSE.

1. INTRODUCTION

In the industry, the control of systems is essential to guarantee a safe and efficient use of resources, with level plants being one of the most common in this sector. In this way, the CE105 MV tank system [1], available in the laboratories of the Surcolombiana University, was studied.

During process control, the possibility of having a mathematical model that adequately represents its dynamics is normally considered, in order to design its respective controller.

In these mathematical models there is an uncertainty factor for each of its parameters. In addition to this, the CE105 MV tank system has a non-linear dynamic behavior. Therefore, the transfer function obtained is simply a linearization at a specific setpoint.

There is much documentation on classic and advanced control techniques applied to liquid level processes. In this contribution, the Internal Model Control (IMC) is used to setpoint tracking and disturbance rejection. Then a comparison is made with the classic PI control to demonstrate the effectiveness of the proposed control. The performance of these controllers is tested and evaluated in a simulation environment. Simulation is done using Matlab®/Simulink® software.

2. MATERIALS AND METHODS

2.1 Process Model

As can be seen in Figure-1, the equipment is represented as a small-scale version of an industrial system or also as a complement to a more complex plant.

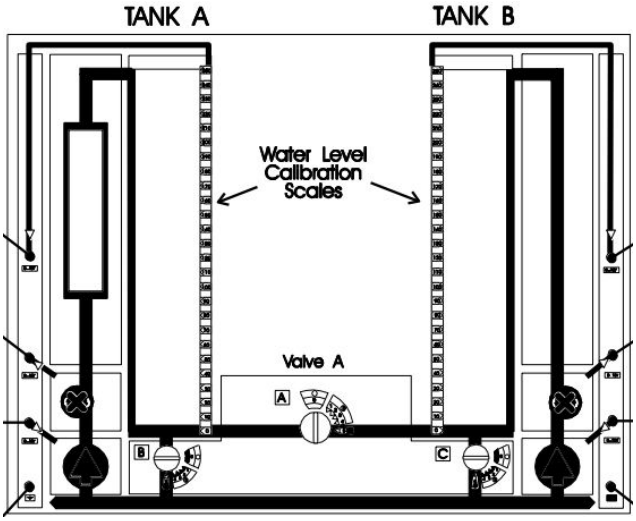

Figure-1. CE105MV system.

There are abundant academic papers on level plant control, either using classical or advanced control techniques [2] - [8]. In this contribution, it is necessary to choose a setpoint in the dynamic model of the system and then approximate it to a transfer function, so that optimal control is performed around the selected setpoint for the controllers to be designed.

For the work, a liquid level tank is considered in configuration of a Single-Input Single-Output system (SISO), as can be seen in Figure-2.

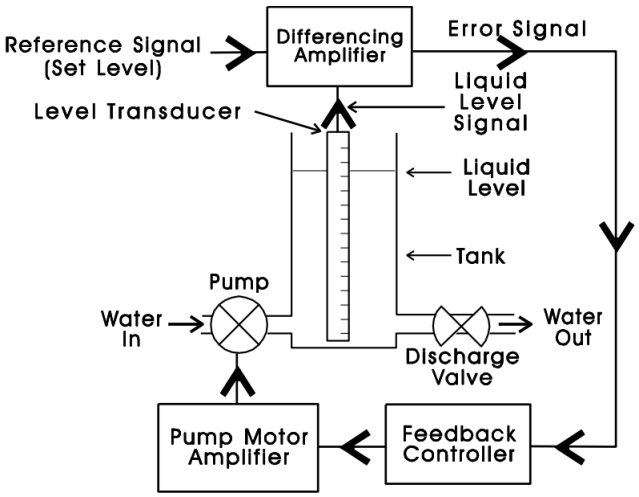

Figure-2. Liquid level plant.

The mathematical model presented is given by the equations that describe the complete system. Figure-2 shows its respective scheme. The dynamic model is determined by the relationship between the input flow $q_i(t)$ and the output flow $q_o(t)$ through the discharge valve [9]. Equation (1) describes this relationship.

$$q_i(t) - q_o(t) = \dot{V}(t) = A\dot{h}(t) \quad (1)$$

$V(t)$ is the volume of the tank, A is the cross-sectional area of the tank and $h(t)$ is the liquid level to be controlled. The output flow through the discharge valve is related to the level of liquid in the tank by (2):

$$q_o(t) = a_v C_v \sqrt{2gh(t)} \quad (2)$$

a_v is the cross-sectional area of the valve orifice, C_v is the discharge coefficient of the valve and g is the gravity constant. Combining (1) and (2) gives:

$$\dot{h}(t) + a_v C_v \sqrt{2gh(t)}/A = q_i(t)/A \quad (3)$$

The input flow is related to the voltage applied to the pump in a linear manner, by means of (4):

$$q_i(t) = K_b v_i(t) \quad (4)$$

K_b is the gain of the pump and $v_i(t)$ is the input voltage of the system. Finally, (5) shows a non-linear relationship between the input voltage $v_i(t)$ and the liquid level inside the tank $h(t)$.

$$\dot{h}(t) + a_v C_v \sqrt{2gh(t)}/A = (K_b/A) v_i(t) \quad (5)$$

Although the water enters the tank from the bottom, the dimensions of the system are small enough so that no delay in the change of level is observed. The values of the system parameters are shown in Table-1.

Table-1. System parameters [1].

Symbol	Description	Value
A	Cross-sectional area of the tanks	$9350\text{x}10^{-6}$ m^2
a_v	Cross-sectional area of the valve orifice	$78.50\text{x}10^{-6}$ m^2
C_v	Discharge coefficient of valve	0.5
h_{max}	Maximum liquid level	0.25 m
v_{max}	Maximum input voltage	10 V
K_b	Pump gain	$6.66\text{x}10^{-6}$m^3 /sV
g	Gravity constant	9.8 m/s^2

The non-linear dynamics (5), must be linearized before PI and IMC control can be applied. The linearization was made using the first order Taylor expansion around the equilibrium point $h^* = 0.1$ m. For the equilibrium point: $f(v_i^*, h^*) = 0$. Linearizing the tank dynamics yields the following transfer function:

$$\frac{\bar{h}(s)}{\bar{v}_i(s)} = \frac{0.00035615}{s+0.01175} \quad (6)$$

2.2 PI Controller Design

The classic structure of a closed-loop feedback controller is represented in Figure-3 [10].

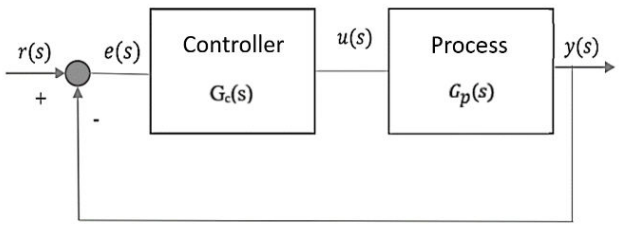

Figure-3. Schematic of a controlled process.

A $G_p(s)$ process is observed with an input $u(s)$ and an output $y(s)$. The output is fed back to compare with the required parameter $r(s)$ and generates an error $e(s)$. This error feeds the controller $G_c(s)$ that manipulates the process. $G_c(s)$ can be a PI-type controller or a PID.

An important feature in controller design is the ability to define virtually meaningful specifications, which will guide the designer through the adjustment process. These specifications should become graphic constraints that facilitate the work of designing [11]. Some of the traditional design specifications are the gain margin and the phase margin [12].

On the other hand, the most practical specifications that any user can easily interpret are the settling time, and the overshoot of the closed-loop response, and of course the robustness of the design. These

criteria are used in this section for the construction of the PI controller.

The algorithm that describes the behavior of the PI controller is presented in (7):

$$u(t) = K_p e(t) + K_i \int_0^t e(t)d\tau \quad (7)$$

$u(t)$ is the output signal of the PI controller, which in this case corresponds to the voltage applied to the pump. $e(t)$ is the input signal of the PI controller, which is defined as $e(t) = r(t) - y(t)$, where $r(t)$ is the setpoint and $y(t)$ is the output of the process, that is, the level of liquid in the tank. K_p is the proportional gain and K_i is the integral gain.

Applying the Laplace transform to (7), the transfer function of the PI controller is found:

$$U(s)/E(s) = K_p + K_i/s \quad (8)$$

Starting from the transfer function at the setpoint (6), and from the intrinsic characteristics in the behavior of the plant, the PI controller parameters are found, so that the closed-loop system meets the following specifications: overshoot of 0 % and a minimum robustness of 0.6.

$$K_p = 99.3282\,,\ K_i = 1.1671 \quad (9)$$

The transfer function of the obtained controller, and the new features provided by it are 0% overshoot and 0.9 robustness.

$$PI(s) = \frac{99.3282\,s+1.1671}{s} \quad (10)$$

2.3 IMC

An IMC controller presents the structure of Figure-4.

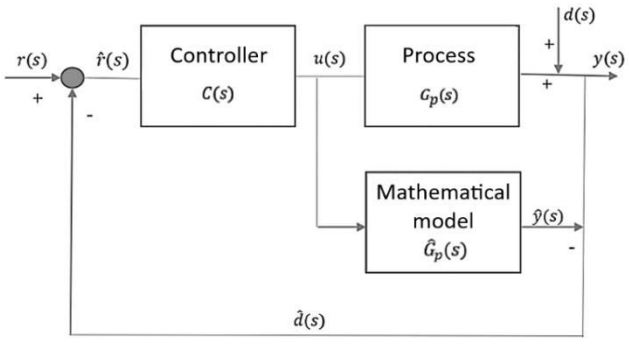

Figure-4. Schematic of an IMC.

The IMC structure has a mathematical model $\hat{G}_p(s)$ in parallel to the plant $G_p(s)$ with the same input $u(s)$ producing an output $\hat{y}(s)$, which will be subtracted from the output $y(s)$ of the plant obtaining a signal $\hat{d}(s)$. This is fed back and compared to the required parameter $r(s)$ to supply the controller $C(s)$ using the signal $\hat{r}(s)$.

Commonly, the IMC defines its bases in the inverse use of the mathematical model of the process, with the aim of obtaining robust control [13] - [14]. In this way the differences between the real plant $G_p(s)$ and its approximate mathematical model $\hat{G}_p(s)$ (6) are reduced. In addition, non-measurable disturbances are monitored.

If $G_P(s) = \hat{G}_p(s)$ and $d(s) = 0$, both the input voltage and the non-measurable disturbances considered in the design will return to the controller by means of feedback generating permanent control of the system.

The following equations describe the IMC controller in Figure-4.

$$y(s) = G_p(s)u(s) + d(s) \quad (11)$$

$$\hat{y}(s) = \hat{G}_p(s)u(s) \quad (12)$$

$$\hat{d}(s) = y(s) - \hat{y}(s) + d(s) \quad (13)$$

$$\hat{r}(s) = r(s) - \hat{d}(s) \quad (14)$$

With $y(s) = G_p(s)u(s)$, $u(s) = \hat{r}(s)C(s)$, and taking into account the disturbances, the output can be expressed as follows:

$$y(s) = G_p(s)C(s)r(s) \quad (15)$$

To achieve zero steady-state error, the condition $y(s) = r(s)$ must be met. When approached by means of (11) the multiplication between $G_p(s)$ and $C(s)$ must be equal to one. To obtain the function that satisfies this product, $C(s)$ must be equal to the inverse of the plant, as shown below:

$$C(s) = \frac{1}{G_p(s)} = G_p(s)^{-1} \quad (16)$$

By inverting the plant model (6), the controller required by the IMC model is obtained:

$$C(s) = \frac{s+0.01175}{0.00035615} \quad (17)$$

The transfer function of the controller must be its proper or semi-proper, that is, the degree of the denominator must be greater than or equal to the degree of the numerator, respectively. From the new configuration obtained (15), it is possible to deduce that it is an improper function, for this reason, the implementation of the filter $f(s)$ is carried out:

$$f(s) = \frac{1}{(\lambda s+1)^n} \quad (18)$$

n is selected, so that when multiplied with $C(s)$ a semi-proper or proper function is obtained. λ is a closed-loop response speed tunning parameter, with a small value for a fast system response and a large value for a slowdown.

For the choice of parameters, the intrinsic physical characteristics of the function plant are considered (6). In which the values $n = 2$ and $\lambda = 10$ are obtained.

$$f(s) = \frac{1}{(10s+1)^2} \quad (19)$$

The filter converts equation (16) into a proper function as follows:

$$C(s) = f(s)\hat{G}_p(s)^{-1} \quad (20)$$

$$C(s) = \frac{s+0.01175}{0.00035615}\left(\frac{1}{(10s+1)^2}\right)$$

$$C(s) = \frac{s+0.01175}{0.03562s^2+0.007123s+0.0003562}$$

Therefore, from (11), the closed-loop response of the system is:

$$y(s) = \frac{0.00035615}{s+0.01175}\left(\frac{s+0.01175}{0.00035615(10s+1)^2}\right)r(s) \quad (21)$$

$$y(s) = \left(\frac{1}{(\lambda s+1)^n}\right)r(s) = \left(\frac{1}{(10s+1)^2}\right)r(s)$$

3. RESULTS AND DISCUSSIONS

The simulation was conducted towards two scenarios to compare the behavior of the PI and IMC controllers. The performance of the controllers is evaluated for the response at the selected setpoint ($H_2 = 0.1$), the tracking to a reference level, and the effective rejection of the disturbances.

3.1 Scenario 1: Disturbance Rejection

Figure-5 evaluates the performance of the controlled system when disturbances are applied. It begins by setting the setpoint so that the output has a value of 0.1 m, and thus the system after being started, a disturbance is performed on it, every 300s.

These disturbances consist of a change in the valve coefficient C_v from 0.2 to 0.4, so that its initial value is subsequently resumed.

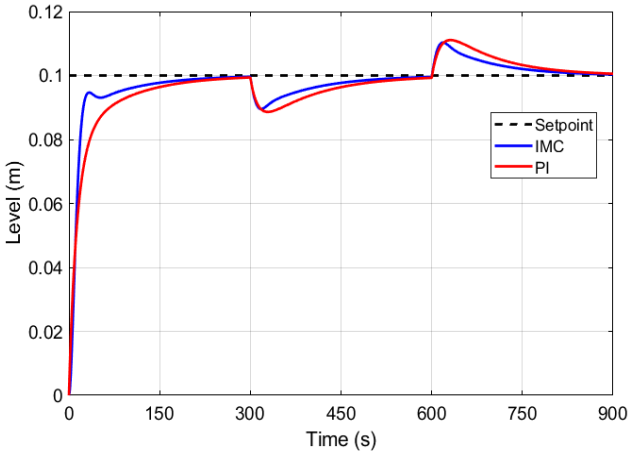

Figure-5. Disturbance rejection with PI and IMC.

Initially, for both cases, the response does not present an overshoot. The system with IMC control has the best settling time with 158 seconds, while the one controlled by the PI has 200 seconds. After this time, the system is disturbed by decreasing its level, by varying the valve discharge coefficient from 0.2 to 0.4.

To counteract these alterations, the controllers increase the control effort to compensate for this decrease. In this way the system is stabilized again, as shown in Figure-6.

Subsequently, after 600 seconds the valve discharge coefficient returns to its initial position of 0.2, generating an increase in the level for the controlled systems. The controllers again adjust the voltage applied to the system, decreasing the level to the value of 0.1 m. Once these results are obtained, it is determined that the IMC controller is the one that offers the best transient response and the most adequate robustness for the selected setpoint.

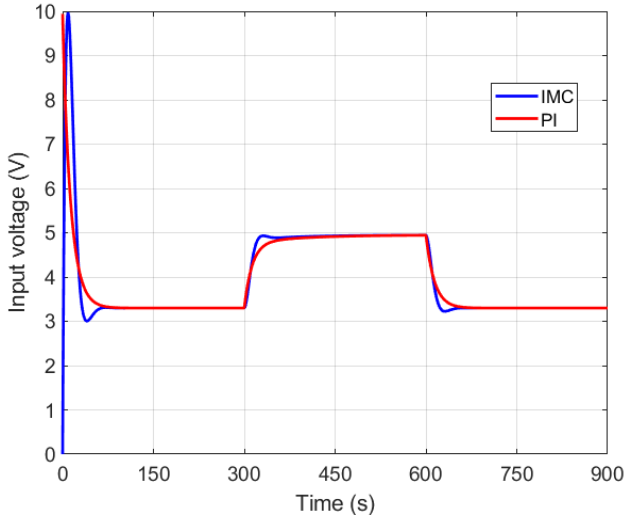

Figure-6. Input process for disturbance rejection with PI and IMC.

3.2 Scenario 2: Setpoint Tracking

To evaluate how the system behaves in a closed loop at different operating points, a reference signal composed of 4 steps with amplitudes of 0.04, 0.08, 0.12, and 0.16m is applied to the system. Figure-7 shows how the process output tracks the setpoint for the linearized equation at 0.1 m.

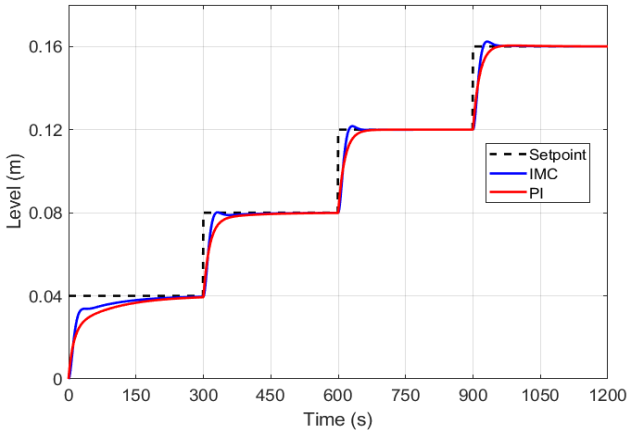

Figure-7. Setpoint tracking with PI and IMC.

As can be seen, the second and third steps have the fastest responses for setpoint tracking, since these setpoints are the closest to the value used for the linearization of the plant's dynamic model. As soon as the setpoint is further away from the design point, the results begin to worsen with overshoot or slow speed in the response.

The results generated by the PI controller are observed. The output tracks the setpoint changes in the same way as the IMC, but with less speed. However, it visibly exhibits better behaviors for setpoints as they move away from the linearization zone chosen for the design, demonstrating greater robustness.

Finally, Figure-8 shows the control effort of both controllers for the setpoint tracking.

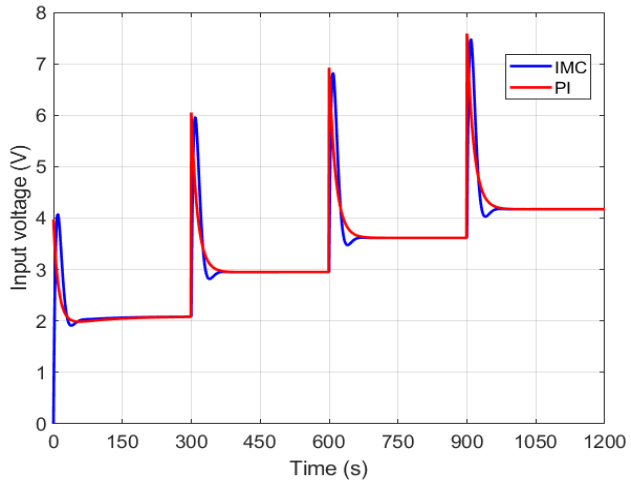

Figure-8. Input process for setpoint tracking with PI and IMC.

To have a more precise comparison of both control strategies, the Root Mean Square Error (RMSE) variation was applied to the 2 proposed scenarios.

$$RMSE = \sqrt{\frac{\sum_{t=1}^{N}[r(t)-y(t)]^2}{N}} \quad (22)$$

where $r(t)$ is the setpoint signal, $y(t)$ is the output signal, and N is the number of samples. Table-2 shows the RMSE variations for both the PI and IMC controllers when the two simulation scenarios are applied.

Table-2. RMSE Variations for PI and IMC.

Scenario	PI (%)	IMC (%)
1	1.16	1.07
2	0.72	0.69

In scenario 1, IMC presents a better performance in the behavior of the plant, results that are ratified again in scenario 2; standing out for the tests carried out near the linearized setpoint. On the other hand, the PI control provides close results that show its great operation and competitiveness compared to other more advanced control methods.

Although different methods were used to control a specific point of the plant, it is noteworthy that the intrinsic characteristics of the plant such as dead time, or minimum phase system, will prevail in the system.

4. CONCLUSIONS

The performance of the IMC and PI control methods was evaluated. The IMC is more effective at fixed setpoints for which it was designed, rejecting disturbances and generating an improvement in the system in terms of transitory and overshoot. This is because it uses an optimal design in the control due to the mathematical estimation of its model and the comparison with the real one.

Since PI also uses the mathematical model, but does not make a comparison with the real plant, it generates good results for monitoring different setpoints, forcing more effort on the controller to process the changing results in each reference; but offering an optimal performance from the analyzed aspects.

In general, the use of the exposed methods is determined by the need for plant control, whether a fixed setpoint or more general control is required. The type of plant to be managed and the operation it performs are also important; what determines if it requires a more advanced and robust technique or a classic one.

REFERENCES

[1] 2016. CE105 and CE105MV Coupled Tanks user manual, primera edición, TecQuipment. pp. 11-13, 29-31.

[2] D. F. Sendoya-Losada, J.D Quintero-Polanco. 2018. Control of yaw angle in a miniature helicopter. ARPN Journal of Engineering and Applied Sciences. 13(2): 620-626.

[3] D. F. Sendoya-Losada, J.D Quintero-Polanco. 2018. PID controller applied to an unmanned aerial vehicle. ARPN Journal of Engineering and Applied Sciences. 13(1): 325-334.

[4] D. F. Sendoya-Losada, J.D Quintero-Polanco. 2018. Design and validation of a PID auto-tuning algorithm. ARPN Journal of Engineering and Applied Sciences. 13(11): 3797-3802.

[5] D. F. Sendoya-Losada. 2018. KCR PID auto-tuner algorithm applied to a FOT device. ARPN Journal of Engineering and Applied Sciences. 13(7): 2505-2510.

[6] A. K. Shah, M. Anilkumar, N. Parikh. Performance analysis of IMC based PID controller tuning on approximated process model. Nirma universitty journal of engineering and technology. 1(2): 1-3.

[7] M. U Khalid and M. D. Kadri. 2012. Liquid level control of nonlinear coupled tanks system using linear model predictive control. IEEE International Conference on Emerging Technologies (ICET). pp. 1-5.

[8] J. Currie and D. I. Wilson. 2010. Lightweight model predictive control intended for embedded applications. IFAC proceedings. 43(5): 278-283.

[9] D. F. Sendoya-Losada, J. O. Arroyave-Quezada and y A. J. Velazquez-Pobre. 2019. EPSAC and NEPSAC Algorithms Applied to a Nonlinear Liquid Level System. en Colombian Conference on Automatic Control (CCAC). pp. 1-5.

[10] R. F. Portilla-Flores. 2017. Diseño e implementación de un control adaptativo para temperatura de un motor de combustión interna utilizando la técnica de identificación basada en mínimos cuadrados recuersivos, Projecto de investigación y desarrollo, Ecuador, Universidad Politécnica Salesiana.

[11] R. D. K. y S. Ionescu. 2006. FRtool: A Frequency Response Tool for CACSD in Matlab®. en IEEE-CACSD'06 International Symposium on Computer-Aided Control Systems Design, Munich, Germany. pp. 1-3.

[12] N.S. Nise. 1995. Control Systems Engineering. 2da edición, Addison-Wesley, capítulo 10.

[13] R. De Keyser. Internal Model Control: IMC. Ghent University.

[14] B. W. Wayne 2002. Bequette Process Control: Modeling, Design, and Simulation, primera edición, Prentice Hall PTR. pp. 330-336.

[15] M. Essahafi. 2014. Model predictive control (MPC) applied to coupled tank liquid level system. arXiv preprint arXiv: 1404.1498.

[16] A. Shehu, and N. A. Wahab. 2016. Applications of MPC and PI controls for liquid level control in coupled-tank systems. IEEE International Conference on Automatic Control and Intelligent System (I2CACIS). pp. 119-124.

[17] S. Banerjee, S.Das, S.Khatua, A. Gupta, P. Arvind, S. Kumari. 2017. Liquid level control system using observer based constrained discrete-time model predictive control. IEEE International Conference on Circuit, Power and Computing Technologies (ICCPCT). pp. 1-8.

[18] A. Shehu and N. A. Wahab. 2016. Applications of MPC and PI controls for liquid level control in coupled-tank systems. IEEE International Conference on Automatic Control and Intelligent System (I2CACIS). pp. 119-124.